

A MODEL FOR THE HIGH TEMPERATURE TRANSPORT PROPERTIES OF HEAVILY DOPED P-TYPE SILICON-GERMANIUM ALLOYS. c.B. Vining, 1994

CRONIN B. VINING

Jet Propulsion Laboratory, California Institute of Technology, Pasadena,
CA 91109

ABSTRACT

A model is presented for the high temperature transport properties of large grain size, heavily doped p-type silicon-germanium alloys. Good agreement with experiment ($\pm 10\%$) is found by considering acoustic phonon and ionized impurity scattering for holes and phonon-phonon, point defect and hole-phonon scattering for phonons. Phonon scattering by holes is found to be substantially weaker than phonon scattering by electrons, which accounts for the larger thermal conductivity values of p-type silicon-germanium alloys compared to similarly doped n-type silicon-germanium alloys. The relatively weak scattering of long-wavelength phonons by holes raises the possibility that p-type silicon-germanium alloys may be improved for thermoelectric applications by the addition of an additional phonon scattering mechanism which is effective on intermediate and long-wavelength phonons. Calculations indicate improvements in the thermoelectric figure of merit up to 40% may be possible by incorporating several volume percent of 20 Å radius inclusions into p-type silicon-germanium alloys.

INTRODUCTION

Silicon-germanium (SiGe) alloys are the current material of choice for the active elements in radioisotope thermoelectric generators (RTG's)¹ which provide reliable electrical power for the Voyager and Galileo spacecrafts. Recent improvements in thermoelectric figure of merit values² ensure that these materials will play a vital role in space power systems for some time to come. Since even modest improvements in thermoelectric performance can result in substantial savings due to the high cost of fuels for RTGs, better theoretical models for their transport properties would be very useful.

The purpose of this study is to develop a physically reasonable model for the high temperature properties of p-type SiGe alloys which treats all of the transport properties on a reasonably consistent footing. An essentially similar model has been recently developed for n-type SiGe alloys³, and the present model is closely patterned after that work. Such

Vining

1 of 10

models provide a baseline for examining the potential for improving the performance of the material through various modifications, such as doping optimization and by the incorporation of phonon scattering centers.

Fortunately, the physical understanding of transport in silicon and SiGe alloys is relatively mature. A model is available for the mobility of p-type silicon^{4,5} which accurately reproduces the mobility and resistivity of p-type silicon over a wide range of temperature and doping levels. Some calculations are available for the mobility of SiGe alloys as well.^{6,7,8} Detailed models for the thermal conductivity of SiGe alloys are available for low temperatures,⁹ high temperatures and high doping levels,^{10,11} and have been extended to include the effects of grain boundary scattering.¹²

Typically these models emphasize only a single transport property and by including various effects eventually find good agreement with experiment for some set of parameters which define the model. However, no published model simultaneously accounts for the high-temperature Seebeck coefficient (Q), electrical resistivity (ρ), Hall mobility (μ_H), and thermal conductivity (k) for p-type SiGe alloys over the entire range of temperatures and doping levels of interest to thermoelectric applications.

This paper describes a predictive, quantitative, theoretically justifiable model of all the thermoelectric properties of SiGe alloys. The model has also been extended to consider the effect of small, chemically inert inclusions on the thermoelectric properties.

DESCRIPTION OF THE MODEL

The transport properties are calculated using essentially the same model developed previously for n-type SiGe and described in detail reference 3. There are, however, several important differences between the n-type model and the current model for p-type SiGe.

The first significant change results from the three valence bands of p-type SiGe, while the previous model for n-type SiGe considered only one conduction band and one valence band. In principle all three valence bands should be considered, but it was found in this study that all of the transport properties of p-type SiGe could be reasonably well described by using only a two-valence band model. Thus, the transport expressions in reference 3 labeled '-' and '+' for electrons and holes, respectively, should be generalized to an index, i , which indicates whether the expression refers the single conduction band or one of the two valence bands considered in this case.

Each of the total transport coefficients are now represented by sums over each of the three bands. The expression for the total Lorenz number

(equation 19 from reference 3) changes form slightly and now becomes:

$$L = \left[\sum_i L^i \sigma^i + \frac{1}{2} \sum_{ij} \frac{\sigma^i \sigma^j}{\sigma} (Q^i - Q^j)^2 \right] / \sigma$$

where the indices i and j run over each of the three bands. Also, the parameters entering the charge carrier relaxation time expressions (equations 22 and 23 from reference 3) are now different for each band.

A second significant change in the present model stems from the anticipation that lattice thermal conductivity reduction techniques are of some interest. The previous calculation of the lattice thermal conductivity considered that phonons may be scattered by 1) other phonons, 2) point defects and 3) charge carriers. However, for $\text{Si}_{0.8}\text{Ge}_{0.2}$ point defect scattering alone reduces the phonon mean free path ($l = v\tau_c$) to 0.64 Å for the highest energy phonons (i.e. phonons with energy = $k_B\theta$). Such a short mean free path is physically unreasonable, since it is much less than either the phonon wavelength (4.4 Å) or the interatomic spacing (2.7 Å). Consequently, some cutoff must be imposed on the phonon scattering rate. In this study, the phonon scattering rate is therefore given by equation 34 of reference 3 or by $\tau_c^{-1} = v/a$ (where a is the interatomic spacing), whichever is smaller.

A third change reflects the greater stability of boron doped SiGe compared to phosphorus doped SiGe. Dopant precipitation and re-resolution occurs at a much slower rate for boron compared to phosphorus and therefore the boron content can be considered fixed for each sample, even as a function of temperature. This greatly reduces the number of adjustable parameters compared to n-type SiGe, where the phosphorus content varies as a function of temperature, even during a single determination of the transport properties.

A final difference between this and the previous model involves the deformation potential characterizing the carrier-phonon interaction. In the previous model, the same value for the deformation potential was found to describe both the electron-phonon scattering rate and the phonon-electron scattering rate (equations 22 and 33 of reference 3) reasonably well. For p-type SiGe, this was found not to be the case. Use of the same deformation potential for both scattering rates either over-estimated the effect of doping on the thermal conductivity, or underestimated the effect of doping on the hole mobility. Therefore, different deformation potentials were used to describe the two scattering rates.

Writing
 for
 10

NUMERICAL DETAILS

The fitting procedure has been described previously.³ Experimental data were taken from several sources, which are summarized in Table I. The data cover a composition range from pure silicon to $\text{Si}_{0.6}\text{Ge}_{0.4}$, carrier densities from 10^{14} to $5 \times 10^{20} \text{ cm}^{-3}$, temperatures from 300 to 1200 K, and represents 297 independent measurements of transport coefficients with 244 degrees of freedom, for the determination of 53 adjustable parameters, 47 of which represent the doping levels of the samples listed in Table I. All of the data used in this study were determined on single crystal or zone-leveled materials.

Table I. Experimental data on p-type SiGe alloys

Number of Samples	Composition range $\text{Si}_{1-x}\text{Ge}_x$	Doping range (cm^{-3})	Temperature range (K)	Data Available
1 ¹³	0.0	2.8×10^{19}	300-1000	σ, μ_H
8 ¹⁴	0.0	8×10^{18} - 1.8×10^{20}	300	σ, μ_H
5 ¹⁴	0.0	1×10^{14} - 1×10^{17}	300	σ, μ
7 ¹⁵	0.15-0.3	3.4×10^{19} - 3.5×10^{20}	300-1200	σ, Q, k
26 ¹⁵	0.15-0.4	5×10^{18} - 5×10^{20}	300	σ, μ_H, Q, k

RESULTS

A single least-squares fit simultaneously applied to all of the data described in Table I resulted in the fit parameters shown in Table II with a root mean square deviation (RMSD) between the calculated and observed values of $\pm 10\%$. Including ionized impurity scattering for the second valance band (which has been neglected here) and re-optimizing all of the parameters only improved the RMSD by less than 0.5%, resulted in an un-physically large value for this dielectric constant ($\epsilon_2 \approx 90$) and removed no systematic errors. So, this effect has been neglected. Calculating phonon scattering rates using the same deformation potentials for phonon-carrier scattering and carrier-phonon scattering resulted in a RMSD $\approx \pm 24\%$, and systematically underestimated the lattice thermal conductivity and overestimated the mobilities. Therefore, as stated above, different values were used for the various deformation potentials.

Table II. Scattering rate and band parameters from fit to p-type SiGe

parameter	Description	Value from fit
m_1	effective mass for valance band #1	1.054 m_0
E_1	deformation potential for valance band #1	3.109 eV
ϵ_1	dielectric constant for valance band #1	9.805
m_2	effective mass for valance band #2	1.405 m_0
E_2	deformation potential for valance band #2	5.894 eV
E_{phonons}	deformation potential for phonon scattering rate	1.973 eV

The agreement between the calculated and observed properties for $\text{Si}_{0.7}\text{Ge}_{0.3}$ is shown in Fig. 1. The systematic changes in these properties with doping level (represented by the different samples) and temperature are well reproduced. The difference between the calculated and observed values of the thermal conductivity actually never exceeds 11%, but appears exaggerated in Fig. 1 due to the expanded scale used for the thermal conductivity axis.

The agreement between the calculated and observed Hall mobility is shown in Fig. 2. The Hall mobility decreases rapidly with increasing doping from 10^{16} to about 10^{19} cm^{-3} , and decreases at a less rapid rate as the doping level is increased further. This qualitative dependence is reasonably well reproduced by the calculated mobilities, although the absolute values of the calculated mobilities are as much as 20% off from the observed values. Qualitatively, the mobility at the lowest doping levels is determined largely by the first valance band, while the second valance band largely dominates the mobility above about $10^{19} \text{ carriers/cm}^3$.

The dimensionless thermoelectric figure of merit ($ZT = Q^2T/\rho k$) is shown as a function of doping level and temperature in Fig. 3. ZT is a multi-valued function of the Hall hole concentration because at high temperatures and low doping levels the Hall coefficient (R_H) decreases rapidly with the onset of thermal excitation of carriers, resulting in an apparently large Hall carrier concentration, even for a relatively small net carrier concentration. The nearly vertical, dashed line in Fig. 3 represents p-type SiGe doped at a level typical of material used in current RTGs.

This model can be easily extended to examine the effects of various

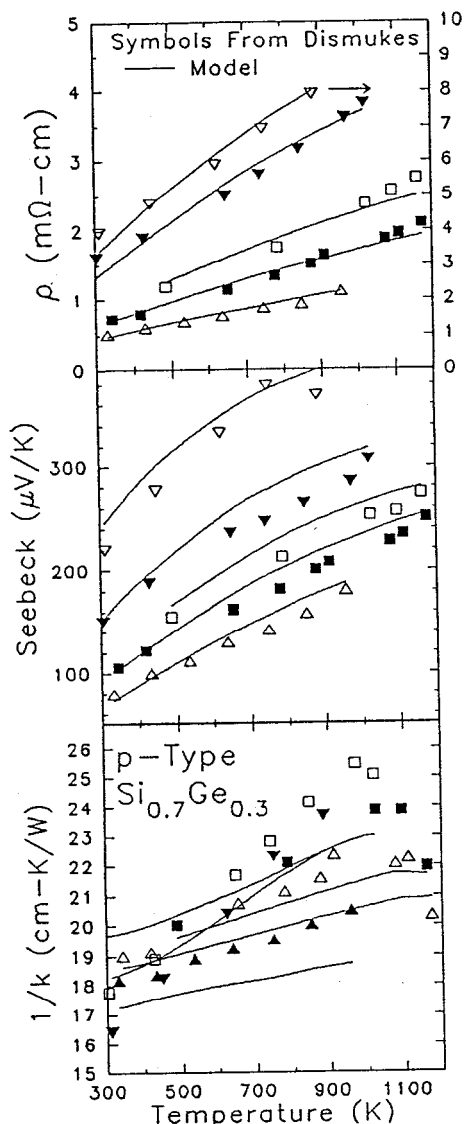


Fig. 1. Resistivity, Seebeck and thermal conductivity for p-type $\text{Si}_{0.7}\text{Ge}_{0.3}$. The points are experimental results and the lines are calculated.

modifications to p-type SiGe. One modification which has been examined is the effect of inclusion of microscopic particles, randomly and uniformly distributed through an otherwise undisturbed lattice of SiGe. Simple expressions have been suggested¹⁶ to describe the effect of such inclusions on the various transport properties. The Seebeck coefficient is taken to be unaffected, which should be valid so long as the inclusions are perfect electrical insulators. The electrical conductivity is taken to be reduced by the factor $(1-4/3 c)$, where c is the volume fraction of the sample occupied by the inclusions. This should be reliable so long as the particles are much larger than the electron mean free path. The main change to the model is the addition of a phonon scattering rate due to the presence of the inclusions given by

$$\tau_{inclusions}^{-1} = \frac{3vc}{4r}$$

where r is the radius of the inclusion and v is the speed of sound in the matrix. This expression should be reasonably reliable so long as the particles are large compared to the wavelength of the phonon.

With these expressions, the effect of microscopic inclusions on the figure of merit can be examined. As a specific example, the figure of merit has been calculated for $\text{Si}_{0.8}\text{Ge}_{0.2}$ at 1050 K, as a function of the size and concentration of inclusions. These results are shown in Fig. 4, where for simplicity only the figure of merit at the optimum doping level is considered. These calculations show that if particles as small as 20 Å in radius can be incorporated in SiGe at the several volume percent level, then improvements in the figure of merit of nearly 40% may be possible.

The reason why ZT is so strongly affected by inclusions is illustrated

in Fig. 5. The lattice thermal conductivity (given more accurately by equations 26-29 of reference 3) can be approximated by

$$k_l = \frac{1}{3} C_v v l$$

where C_v is the specific heat, l is the phonon mean free path

$$l = \int_0^1 \tau v_s x^2 dx$$

and x is the reduced phonon energy. Fig. 5 shows the integrand for the mean free path integral for various combinations of scattering mechanisms. The lattice thermal conductivity is determined by the area under these curves, and a lower curve therefore indicates a smaller lattice thermal conductivity. The line labeled $a_0 x^2$ indicates the minimum thermal conductivity and the integrand is never allowed to be below this curve.

The line labeled 'Normal+Umklapp' represents and ideal, undoped crystal with no defects. Addition of the Si-Ge point defect scattering greatly lowers the integrand, as shown by the curve labeled 'N+U+PD.' Addition of doping alone, however, only lowers the curve at the lowest energies, indicated by the curve labeled 'N+U+holes,' and therefore has a relatively small effect on the thermal conductivity. 20 Å inclusions are seen to be far more effective at lowering the lattice thermal conductivity, as indicated by the curve labeled 'N+U+ 20 Å inclusions.' The total thermal conductivity, indicated

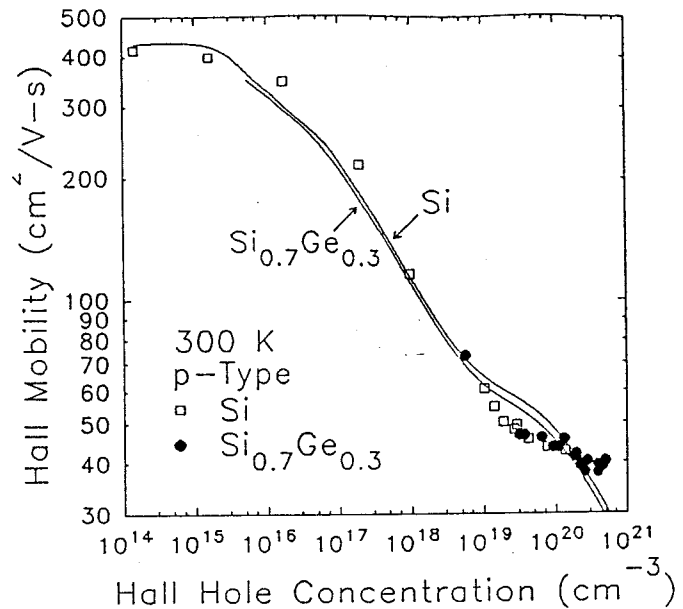


Fig. 2. Hall mobility as a function of the Hall hole concentration (r/eR_H) for p-type Si and $\text{Si}_{0.7}\text{Ge}_{0.3}$. The points are experimental and the lines are calculated.

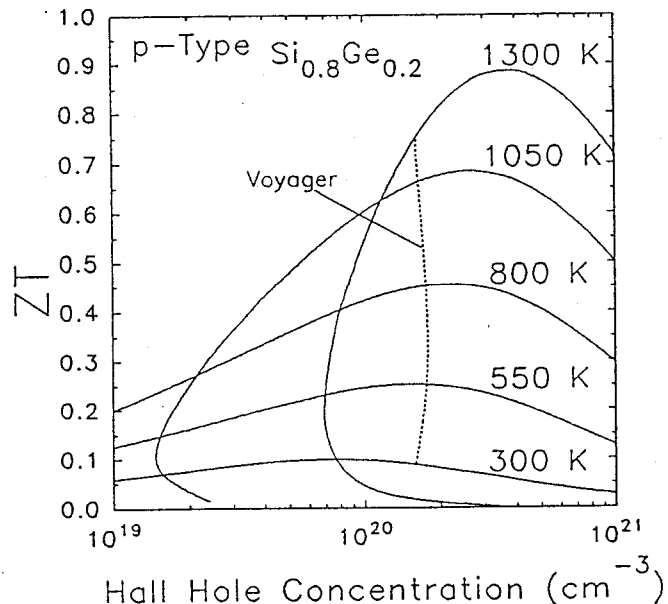


Fig. 3. ZT of p-type $\text{Si}_{0.8}\text{Ge}_{0.2}$ as a function of Hall hole concentration (r/eR_H). The dashed line represents doping levels currently used in RTGs.

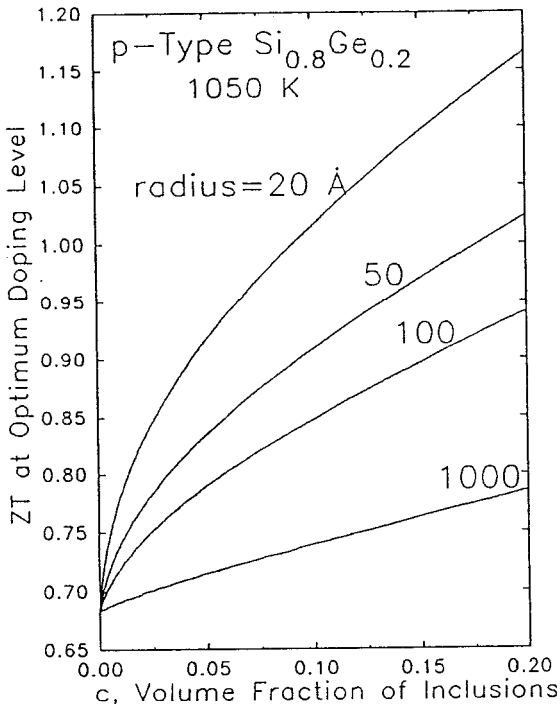


Fig. 4. Optimum ZT as a function of the size and volume fraction of inert inclusions.

by the line labeled 'Total,' is seen to be constrained mostly by the effects of inclusions and point defects.

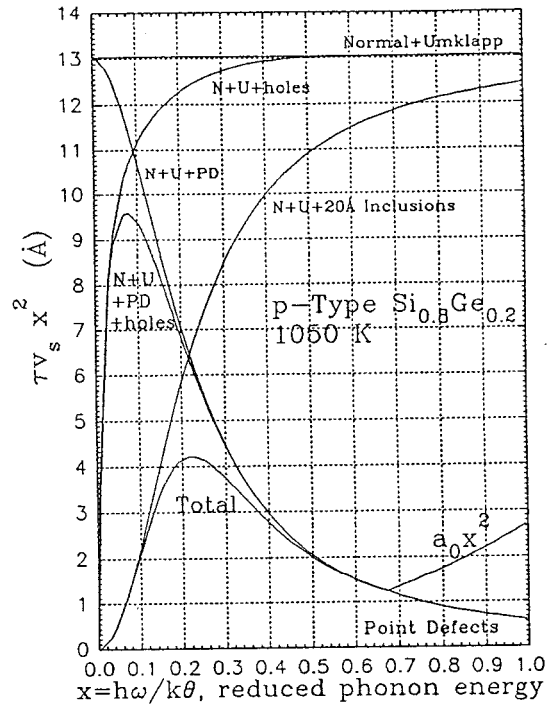


Fig. 5. These plots show the effect of normal (N) and umklapp (U) scattering, point defects (PD), holes, inclusions, and the minimum mean free path ($a_0 x^2$) on k_f .

DISCUSSION AND CONCLUSIONS

The present model provides a good description of the transport properties of p-type SiGe alloys. The parameters which result from the fitting procedure are physically reasonable, although not identical to other estimates of the same parameters. Many effects thought to be important have been neglected here, such as: incomplete ionization of the dopants; scattering of carriers by other carriers, by optical phonons and by neutral impurities; non-parabolic and non-isotropic hole energy dispersion relations, etc. Yet in spite of the neglect of these various effects, all of the qualitative trends are reasonably well reproduced by this model and the quantitative agreement with experiment is quite acceptable.

A significant, systematic discrepancy exists between calculated and observed Hall mobility values, as shown in Fig. 2. Moreover, the effects included in the present model will always calculate a Hall mobility which is somewhat greater than the conductivity mobility. But the experimental and theoretical evidence is very strong¹⁷ that the Hall mobility is actually somewhat less than the conductivity mobility for p-type Si, an effect normally attributed to hole-hole scattering processes and/or non-isotropic hole energy dispersion relations, which have been neglected in this model.

A second concern with the present model involves the use of a

significantly smaller value for the phonon-hole deformation potential compared to the hole-phonon deformation potential. A plausible explanation for this discrepancy may be that some of the hole scattering which this model attributes to interactions with acoustic phonons may actually be due to interactions with optical phonons or interactions with other carriers.

The principal value of this model is that it reproduces qualitatively correctly all of the trends as functions of composition, doping level, and temperature in an internally consistent manner and with reasonable quantitative accuracy. These calculations suggest that slight increases in the boron doping levels may yield increases in ZT in the 3 to 6% range (see Fig. 3) and that further increases of up to 40% may be possible by the addition of microscopic inclusions (as shown in Fig. 4).

ACKNOWLEDGMENTS

The author would like to thank Dr. P. Klemens and Dr. J-P. Fleurial for many helpful discussions related to this work. The work described in this paper was carried out at the Jet Propulsion Laboratory, California Institute of Technology, under contract with the National Aeronautics and Space Administration.

1. G. L. Bennett, J. J. Lombardo, and B. J. Rock, in Proceedings of the 18th International Energy Conversion Engineering Conference, Orlando, FL, 1983.
2. J. W. Vandersande, A. Borshchevsky, J. Parker, and C. Wood, in Proceedings of the 7th International Conference on Thermoelectric Energy Conversion, edited by K. R. Rao (University of Texas, Arlington, TX, 1988), p. 76.
- 3.. C. B. Vining, J. Appl. Phys. 69, 331 (1991).
- 4.. L.C. Linares and S.S. Li, J. Electrochem. Soc. 128. 601 (1981).
- 5.. J.F. Lin, S.S. Li, L.C. Linares, and K.W. Teng, Solid-State Electronics, 24, 827 (1981).
- 6.. A. Amith, in Proceedings of the 7th International Conference on the Physics of Semiconductors, edited by M. Hulin (Academic, New York, 1964) p. 393.
7. S. Krishnamurthy, A. Sher, and A. Chen, Appl. Phys. Lett. 47, 160 (1985).

8. E.V. Khutsishvili, Soobshcheniya Akademii Nauk Gruzinskoi SSR (Bulletin of the Academy of Sciences of the Georgian SSR) 131, 293 (1988).
9. A.M. Toxen, Phys. Rev. 122, 450 (1960).
10. E.F. Steigmeier and B. Abeles, Phys. Rev. 136, A1149 (1964).
11. R.S. Erofeev, E.K. Jordanishvili, and A.V. Petrov, Sov. Phys. Solid State 7, 2470 (1966).
12. C.M. Bhandari and D.M. Rowe, Thermal Conduction in Semiconductors, (Wiley, New York, 1988).
13. This study.
14. W.R. Thurber, R.L. Mattis, Y.M. Liu, and J.J. Filliben, Nat. Bur. Stand. Spec. Publ., 400-64 (1981).
15. J.P. Dismukes, L. Ekstrom, E.F. Steigmeier, I. Kudman, and D.S. Beers, J. Appl. Phys. 35, 2899 (1964).
16. P.G. Klemens and D. White, private communications.
17. J.F. Lin, S.S. Li, L.C. Linares, and K.W. Teng, Solid-State Electronics 24, 827 (1981).